Numerical Study of a Mesoscale Vortex in the Planetary Boundary Layer of the Meiyu Front

SHEN Hangfeng[1,2] (沈杭锋), ZHAI Guoqing[1*] (翟国庆), ZHU Ye[1,3] (朱 业), and XU Yaqin[4] (徐亚钦)

1 *Department of Earth Sciences, Zhejiang University, Hangzhou* 310027

2 *Hangzhou Meteorology Bureau, Hangzhou* 310057

3 *Marine Monitoring and Forecasting Center of Zhejiang, Hangzhou* 310007

4 *Wenzhou Meteorology Bureau, Wenzhou* 325000

(Received December 23, 2011; in final form April 5, 2012)

ABSTRACT

It was found that the heavy rainfall event along the Meiyu front in the lower reaches of the Yangtze River on 23 June 2009 was connected with a mesoscale disturbance vortex, which originated from the planetary boundary layer (PBL) and developed upward later and was discovered by using the Shuman-Shapiro filtering method. The mesoscale disturbance vortex in the PBL (PMDV) in this process corresponded well to the short-time rainstorm in the Doppler radar echo. Analysis of the high-resolution simulation results from the Advanced Weather Research and Forecasting Model (ARW) showed that there were several surface disturbances along the southern warm section of the Meiyu front prior to the generation of the PMDV. The PMDV interacted with the mesoscale convective system (MCS) and intensified the local convective precipitation. The north and southwest flows in the PBL converged at the time of the PMDV formation. Meanwhile, a southwesterly jet on the top of the PBL to the south side of the vortex reinforced the ascending motion and convergence. Hence, it is concluded that the PMDV was generated when the strong cold air flows north of the shear line encountered the southwest flow south of the shear line. The convergence line in the PBL, the intensification of the southwest wind, and the southward aggression of the north wind were critical for the development of the PMDV. The release of latent heat was found crucial for the formation of the PMDV as it facilitated the convergence at low levels.

Key words: PBL, mesoscale vortex, numerical simulation, Meiyu frontal rainstorm, PMDV

Citation: Shen Hangfeng, Zhai Guoqing, Zhu Ye, et al., 2012: Numerical study of a mesoscale vortex in the planetary boundary layer of the Meiyu front. *Acta Meteor. Sinica*, **26**(6), 788-802, doi: 10.1007/s13351-012-0609-y.

1. Introduction

Mesoscale convective systems (MCSs) characterized usually by extensive trailing stratiform regions could modify their local environments with strong and persistent mesoscale circulations rooted in deep layers of diabatic heating and cooling. Sometimes, there are mesoscale convective vortices (MCVs) in these circulations (Johnston, 1981; Raymond and Jiang, 1990; Knievel and Johnson, 2002). MCV was first defined by Zhang and Fritsch (1987) and later by Zhang (1992) as: a significant concentration of positive relative vorticity of magnitude at least that of the local Coriolis parameter, eventually leading to the formation of a closed circulation. Most MCVs have horizontal scales of several hundred kilometers and time scales of hours to days. MCVs are most likely to occur in a weak flow, weak vertical wind shear, weak background relative vorticity, and strong vertical and horizontal moisture gradients (Bartels and Maddox, 1991). MCVs play an important role in organizing convection, reinforcing MCSs, and causing extreme rainfall (Schumacher and Johnson, 2008, 2009).

James and Johnson (2010) investigated 45 MCVs that developed along MCSs and found that 28 (62%) of them were accompanied by mesolows at the sur-

Supported by the National Natural Science Foundation of China (41175047) and China Meteorological Administration Special Public Welfare Research Fund (GYHY201006014 and GYHY201006007).

*Corresponding author: zhaigq@zju.edu.cn.

face, and they could be further categorized into three groups according to the precipitation organization and associated mesolows: rearinflow-jet MCVs, collapsing-stratiform-region MCVs, and vertically coherent MCVs. The remaining 17 (38%) of the cases did not contain a surface mesolow. Two repeating patterns of MCVs for the associated precipitation organization were identified for the remaining 17 cases: remnant-circulation MCVs and cold-pool-dominated MCVs.

For the formation of MCV, various conclusions have been drawn. Some researchers proposed that low-to-mid level convergence was the main cause for the formation of MCV (Zhang and Fritsch, 1988; Menard and Fritsch, 1989; Olsson and Cotton, 1997). Verlinde and Cotton (1990) found that the formation of MCV could result from multiple convective updrafts and tipping, i.e., the convergence at mid levels as well as the tipping of rear-inflow horizontal vorticity (Brandes, 1990; Zhang, 1992; Davis and Weisman, 1994). Bartels and Maddox (1991) pointed out that the convergence acting on planetary vorticity could generate MCV. Cram et al. (2002) showed that the main reason for genesis of an MCV was an earlier convergence followed by a horizontal tipping. Knievel and Johnson (2003) suggested that the strong upper-level tipping coupled with mid-level convergence and weak low-level tipping was the dominating contributor to the generation of MCV.

The middle and lower reaches of the Yangtze River (MLYR) was one of the three main convective areas in China (Tao et al., 1998). The Meiyu frontal heavy rainfall often leads to devastating flooding over the MLYR in warm seasons. The heavy rainfall was usually caused by the MCS and mesoscale vortex which formed, propagated, and organized along the front (Zhang and Tan, 2009). Previous studies showed that there are two kinds of vortex systems associated with the Meiyu front. One was an east propagating southwest vortex and the other was locally generated mesoscale vortex under favorable thermodynamic and dynamic conditions (Sun and Du, 1996; Hu and Pan, 1996; Gao and Xu, 2001; Dong and Zhao, 2004).

For the locally generated mesoscale vortex along the Meiyu front, Zhai et al. (2003) investigated the small scale vortices in the planetary boundary layer (PBL) and found that the mesoscale convergence in the PBL was the initial dynamical condition that triggered the meso-γ-scale vortex. A convergence line appeared prior to the vorticity. Zhai et al. (2007) further pointed out that sometimes several weak small mesoscale vortices in the PBL could form a vortex group along the Meiyu front over the MLYR. They were usually accompanied by surface low trough or mesoscale low centers and were responsible for heavy rainfall.

However, it is usually hard to observe these vortices directly as they are characterized with small spatial scale, short life span and they develop only in the PBL. In this study, we investigate the development and structure of the mesoscale disturbance in the PBL (PMDV) along Meiyu front on 23 June 2009 by employing intensive surface observation data from automated surface observing system and a high-resolution numerical model.

2. Data and method

Several datasets were combined in this study, including (1) 12-h temporal and about 300-km horizontal resolution sounding data, (2) hourly observations by the East China automated surface observing system, (3) 6-h temporal and 20–25-km horizontal resolution regional spectral model (RSM) data compiled by the Japan Meteorological Business Support Center (obtained from the Key Laboratory of Mesoscale Severe Weather, Ministry of Education, Nanjing University), and (4) Jiujiang Doppler radar data.

To reveal mesoscale features more distinctly, the Shuman-Shapiro filtering method (Zhang et al., 2007; Qin, 2010) was used. This filtering method can decompose a meteorological element f into a large-scale element $\overline{f}$ and mesoscale element f'. Hence, f can be rewritten as $f = \overline{f} \pm f'$. Then, if we chose an appropriate filtering coefficient and a filtering algorithm to eliminate undulation, we can obtain a smoothed field. The disturbed field could be obtained through subtr-

action of the smoothed field from the original. A nine-point filter was applied (Fig. 1), which is written as

$$\overline{f}_0 = \left[(1-s_1)(1-s_2)+\frac{s_1 s_2}{2}\right]^2 f_0 + \frac{1}{2}\Big[s_1(1-s_2) + s_2(1-s_1)\Big]\left[(1-s_1)(1-s_2)+\frac{s_1 s_2}{2}\right]\sum_{i=1}^{4} f_i + \frac{1}{4}\Big[s_1(1-s_2)+s_2(1-s_1)\Big]^2 \sum_{i=5}^{8} f_i,$$

where $s_1 = 1/2$ and $s_2 = 2/3$. The lengths of the grid and undulation were set to 100 and 300 km, respectively.

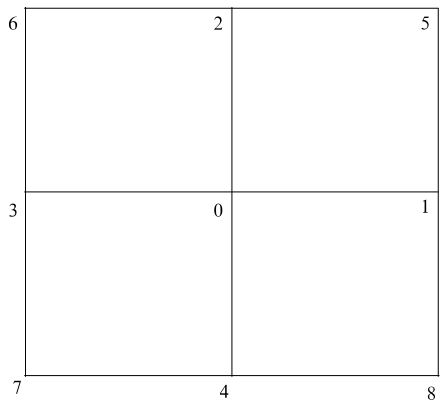

Fig. 1. Grid layout of the nine-point filtering algorithm.

3. Synoptic overview

For the 500-hPa geopotential height field at 0000 UTC 23 July 2009 (Fig. 2a), there were several shortwave troughs (thick dashed line) moving eastward in the westerly wind belt. The cold air associated with the shortwave troughs invaded the MLYR and produced heavy rainfall over parts of Anhui and Zhejiang provinces from 23 to 24 July 2009. Heavy rainfall areas (shaded in Fig. 2b) were located over the south of the Dabie Mountains in Anhui Province and northwestern Zhejiang Province. The rainfall mainly occurred from 2000 UTC 23 to 0400 UTC 24 July 2009. The 24-h precipitation at many stations exceeded 100 mm, and the maximum value reached 197 mm at Dongzhi (DZ) city (black dot in Fig. 2b).

At 0000 UTC 24 July 2009 (Fig. 3a), a confluence line was formed by a northerly flow coming from the west of the low vortex over Jiangsu Province and a westerly flow over Zhejiang Province at 925 hPa in the observed streamline field. A stationary front at the surface (thick solid line) extended from southern Hubei Province and the junction of Anhui and Jiangxi provinces to the middle of Zhejiang Province. There were two southwest low-level jets (marked "J") to the

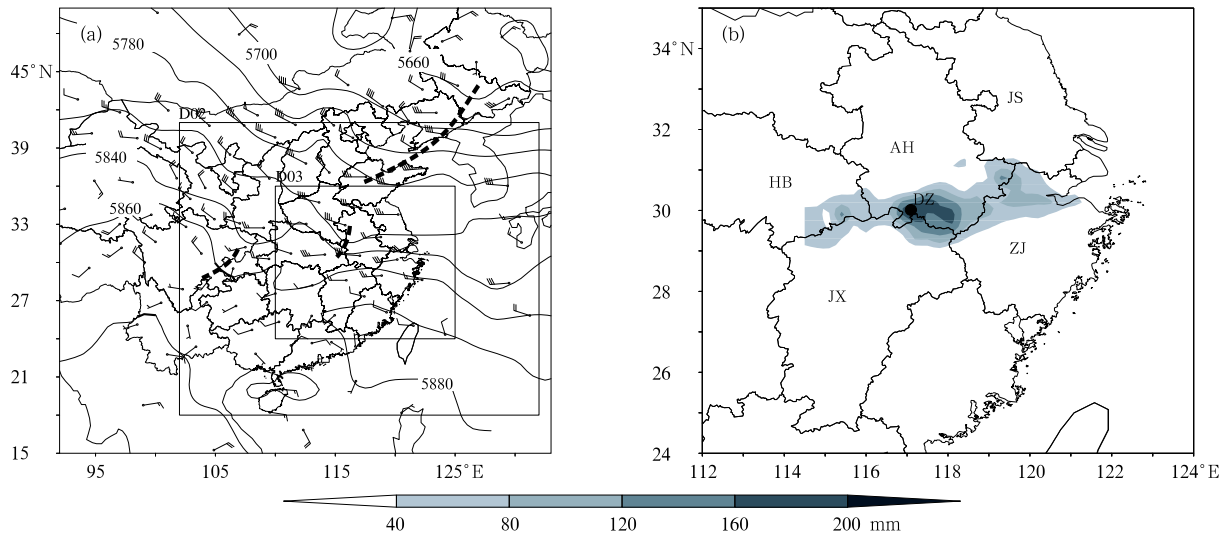

Fig. 2. Observed patterns of (a) 500-hPa geopotential height (contours; gpm) at 0000 UTC 23 July 2009 and (b) 24-h accumulative precipitation (shaded; mm) from 1200 UTC 23 to 1200 UTC 24 July 2009. The thick dashed lines in (a) indicate troughs. ZJ, HB, AH, JS, and JX in (b) represent Zhejiang, Hubei, Anhui, Jiangsu, and Jiangxi provinces, respectively. DZ represents the city of Dongzhi. Boxes in (a) are the nested simulation domains.

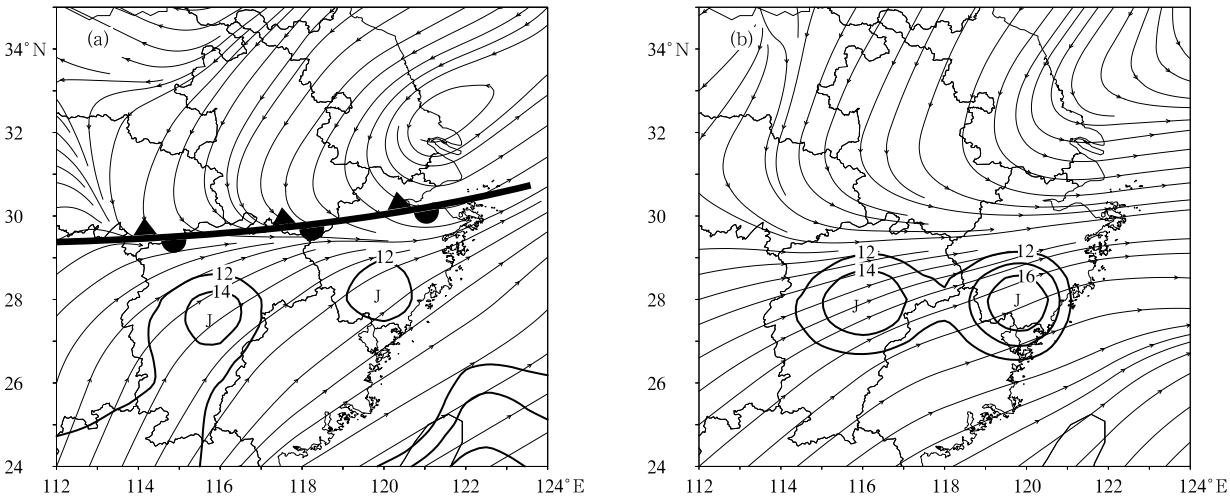

Fig. 3. Observed streamline (fine solid line) and wind speed (thick solid; m s^{-1}) fields based on sounding data at (a) 850 and (b) 925 hPa at 0000 UTC 24 July 2009. "J" represents the center of the jets. The thickest solid line indicates the position of the Meiyu front.

south of the confluence line with axle velocities exceeding 14 m s^{-1}. Heavy rainfall was located just north of the stationary front. The low-level jet (LLJ) and confluence line could also be found at 850 hPa, but there was no low-level vortex over Jiangsu Province.

Typical weather systems associated with the establishment of the Meiyu front and heavy rainfall are shortwave troughs moving eastward, a shear line, a low-level jet (LLJ), and a stationary front at the surface (Zhu et al., 2000). Rainfall is most likely to occur under these favorable large-scale synoptic conditions. Then, following the eastward movement of the low vortex and the southward motion of the shear line, the rainstorm moves from southern Anhui and northern Zhejiang to the coastal area of southeastern Zhejiang, after which it finally dissipates over the sea.

As shown in Fig. 2b, the distribution of the precipitation in the mesoscale rainfall belt was nonuniform. There were several mesoscale rainstorm centers in the rainfall belt. Besides the shear line, MCSs in the Meiyu front could also be connected to these mesoscale rainstorm centers. Previous studies have found that there were usually mesoscale vortices, MCSs, and other mesoscale systems embedded in the shear line of the Meiyu front. These features could directly trigger rainstorms (Yamada et al., 2003).

Figure 3 shows that there were low-level vortices and shear lines in the PBL. However, further analysis is needed to assess whether there were MCSs or mesoscale vortices along the shear line. The Shuman-Shapiro filtering method (Fig. 1) was applied to the 925–850-hPa streamline fields at 0000 UTC 24 July 2009 (Fig. 3), to eliminate the large-scale systems and retain meso- and small-scale systems. Figure 4a shows that a mesoscale vortex (marked "C") of spatial scale less than 100 km was located along the shear line at 925 hPa and it is hereafter called the PMDV in this study. With reference to Fig. 2b, the PMDV is located near DZ city. The next hourly accumulative precipitation with maximum value of 30 mm (shaded in Fig. 4a) appeared around the PMDV. However, there was no vortex on the 850-hPa filtered streamline field near this region (Fig. 4b). Instead, there was a shear line with similar structure to the field before the filtering (see Fig. 3).

The filtering method was also applied to the 6-h temporal and 20–25-km horizontal resolution RSM data at 0000 UTC 24 July 2009. We found that there was a mesoscale vortex near DZ city in the 925-hPa streamline field (Fig. 4c), with a diameter of about 100 km, at the same location as the PMDV in Fig. 4a. Similarly, there was only a shear line, but not a mesoscale vortex in the 850-hPa streamline field at the same time (Fig. 4d).

The mesoscale vortex in Fig. 4 could also be obs-

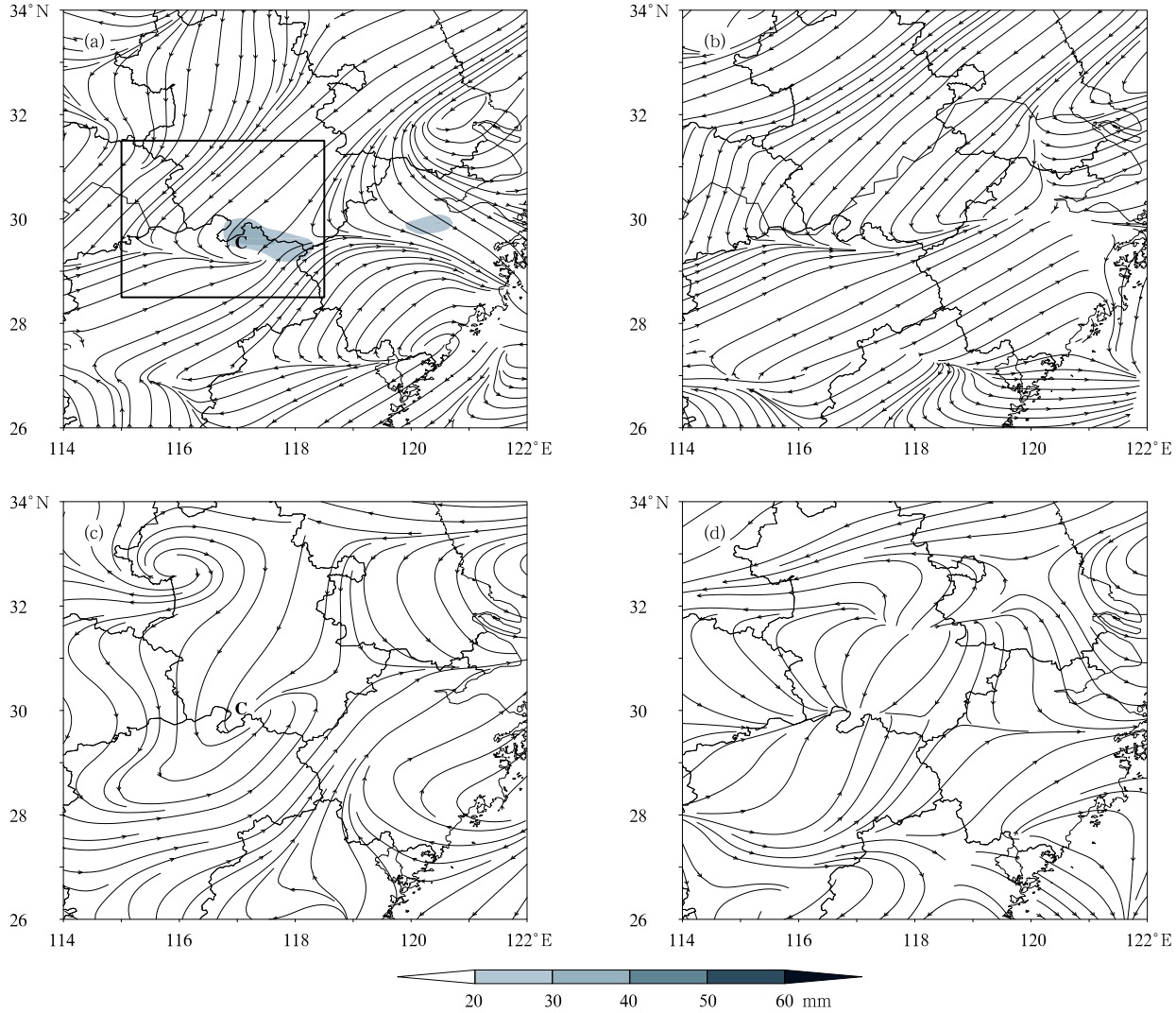

Fig. 4. Filtered streamline fields from (a) 6-h sounding data at 925 hPa, (b) sounding data at 850 hPa, (c) RSM data at 925 hPa, and (d) RSM data at 850 hPa at 0000 UTC 24 July 2009. The shaded area in (a) represents the next hourly precipitation (mm). The symbol "C" indicates the position of the vortex.

erved at lower levels. The surface streamline field (Fig. 5) was analyzed using hourly observations from the East China automated surface observing system.

Figure 5a shows the distribution of the surface weather stations, wind field (barbs), and terrain (contours) at 1800 UTC 23 July 2009, while Fig. 5b shows the surface streamline field at the same time. In Fig. 5b, several surface disturbance vortices can be seen to the south of the Dabie Mountain (DBS) (vortices C_1 and C_2) and between the DBS and Huang mountain (HS) (vortex C_3) prior to the occurrence of the PMDV. The front and the MCS stayed on the northern side, and the surface disturbances occurred on the southern warm section of the Meiyu front. Two hours later (Fig. 5c), the surface vortices gathered gradually as the north wind enhanced and the MCS intensified. Vortex C_1 in Fig. 5b disappeared (it could have dissipated or merged with vortex C_2), but vortex C_3 moved southward and began to influence DZ city. Past hourly accumulative precipitation of 10 mm (shaded) appeared near the DBS and HS, while C_2 and C_3 were staying at the edge of the DBS. Hence, the outflow of MCS may have impacted C_2 and C_3.

With the enhancement of north wind and south-

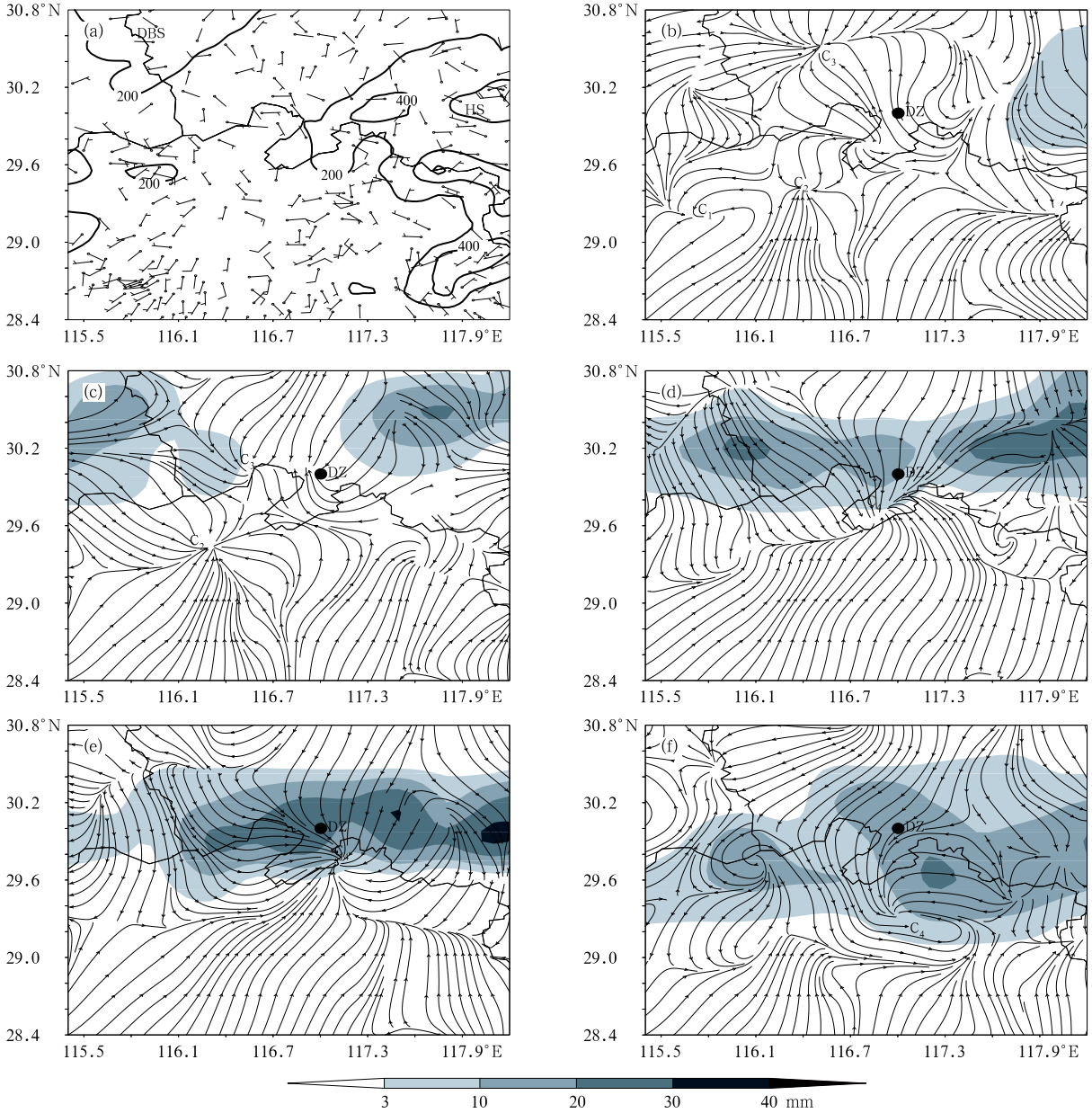

Fig. 5. Distributions of (a) automatic surface weather station wind field and terrain at 1800 UTC and hourly surface streamline field at (b) 1800 UTC, (c) 2000 UTC, (d) 2100 UTC, (e) 2200 UTC 23 July, and (f) 0100 UTC 24 July 2009. The contours in (a) indicate the terrain (m). The shading represents the past hourly precipitation (mm). DBS and HS represent the Dabie and Huang mountains, respectively.

west flow, the surface disturbance vortices became steady. A new vortex C_4 appeared in the vicinity of DZ city. It was likely to have been generated by the merging of C_2 and C_3, as seen from the streamline field at 2100 UTC 23 July 2009 (Fig. 5d). At the same time, rainfall started to intensify and the rainfall centers near HS and DBS in Fig. 5c merged and formed a unified rain belt lying north of C_4. After the formation of C_4, the precipitation in DZ intensified suddenly. At 2200 UTC 23 July 2009 (Fig. 5e), the past hourly accumulative precipitation increased from 10 mm to more than 20 mm. Vortex C_4 remained active for several hours and developed together with the MCS. At 0100 UTC 24 July 2009 (Fig. 5f), the en-

closed structure of C_4 dissipated but C_4 stayed ahead of the rain belt; in the meantime, the PMDV at 925 hPa (Fig. 4a) showed up.

The above analysis revealed that there were several surface disturbances along the southern warm section of the Meiyu front. The surface vortices in the PBL interacted with the MCS. The MCS influenced the initiation of the vortices while the latter intensified the local convective precipitation.

We concluded from the above analysis that there was a mesoscale vortex along the shear line in the PBL during the rainstorm. This disturbance vortex, with a horizontal scale of about 100 km, was generated in the PBL initially and was responsible for the increasingly heavy rainfall over this region.

4. Numerical simulations

In order to analyze in detail the vortex in the PBL, the Advanced Weather Research and Forecasting Model (ARW) version 3.1.1 was employed in this study. The WRF model was a multi-agency effort to build a new generation mesoscale forecast model and data assimilation system. As used in this experiment, WRF is a fully compressible, Euler nonhydrostatic model using a terrain-following hydrostatic-pressure vertical coordinate, with vertical grid stretching such that the vertical levels are closer together near the surface and more spread out aloft. The horizontal grid is an Arakawa C grid. The third-order Runge-Kutta scheme with a smaller time step for acoustic and gravity wave modes is used for numerical integration (Skamarock et al., 2008).

The model adopted the WMS5 microphysics scheme (Hong et al., 2004; Hong and Lim, 2006), and Grell-3D cumulus convection parameterization scheme (Grell and Devenyi, 2002). RRTM scheme (Mlawer et al., 1997) and Dudhia scheme (Dudhia, 1989) were used for long wave radiation and shortwave radiation, respectively. The PBL parameterization followed the Mellor-Yamada-Janjic (MYJ) scheme (Janjic, 1990, 1996, 2002). The model domain covers a coarse mesh (D01) of 45-km grid spacing centered at 30°N, 117°E, a fine mesh (D02) of 15-km resolution, and a finer mesh (D03) of 5-km resolution (Fig. 2a). Because D01 occupies an area larger than that of Fig. 2a, only D02 and D03 are shown in Fig. 2a. Twenty-seven σ levels are set up in the vertical direction. The simulation by the WRF model is started at 0000 UTC 23 July and ended at 1200 UTC 24 July 2009. The NCEP FNL (Final) Operational Global Analysis data are taken as the initial and lateral boundary conditions.

5. Simulation results

5.1 Verification

Figure 6 shows the simulated and observed precipitation. In the observation, the heavy rainfall belt (shaded in Fig. 6a) had a center to the west of the HS, with maximum 24-h precipitation exceeding 190 mm. Another precipitation center was seen in the eastern part of the rain belt, with maximum precipitation of 120 mm located in the HZ area. The simulated 24-h precipitation (contours in Fig. 6a) was generally consistent with the observation. The simulated heavy rainfall had a center to the west of the HS with maximum precipitation of 200 mm. Similarly, a comparison between Figs. 6b and 6c shows that the simulated 3-h precipitation (contours) was similar to the observation (shaded).

The simulated past hourly accumulative precipitation of DZ city (black dot in Fig. 2b) was also compared with the observation (Fig. 7). The observed precipitation (dashed line) increased at 2100 UTC 23 July 2009. It reached a peak of 30 mm at 2300 UTC and thereafter became weaker gradually. The precipitation process was consistent with the surface streamline evolution (Fig. 5). The precipitation of DZ city suddenly intensified at 2100 UTC after the formation of vortex C_4. In the simulation, the preciitation (solid line) increased from 2100 UTC 23 July 2009, peaked at 45 mm at 0000 UTC 24 July 2009, and then weakened gradually. The simulated precipitation was more intense than the observation but lagged by about 1 h.

To highlight the features of the disturbance vortex, we analyzed the simulated mesoscale vortex of the box range shown in Fig. 4a. A distinct mesoscale vortex located southwest of the HS (see Fig. 5a) on

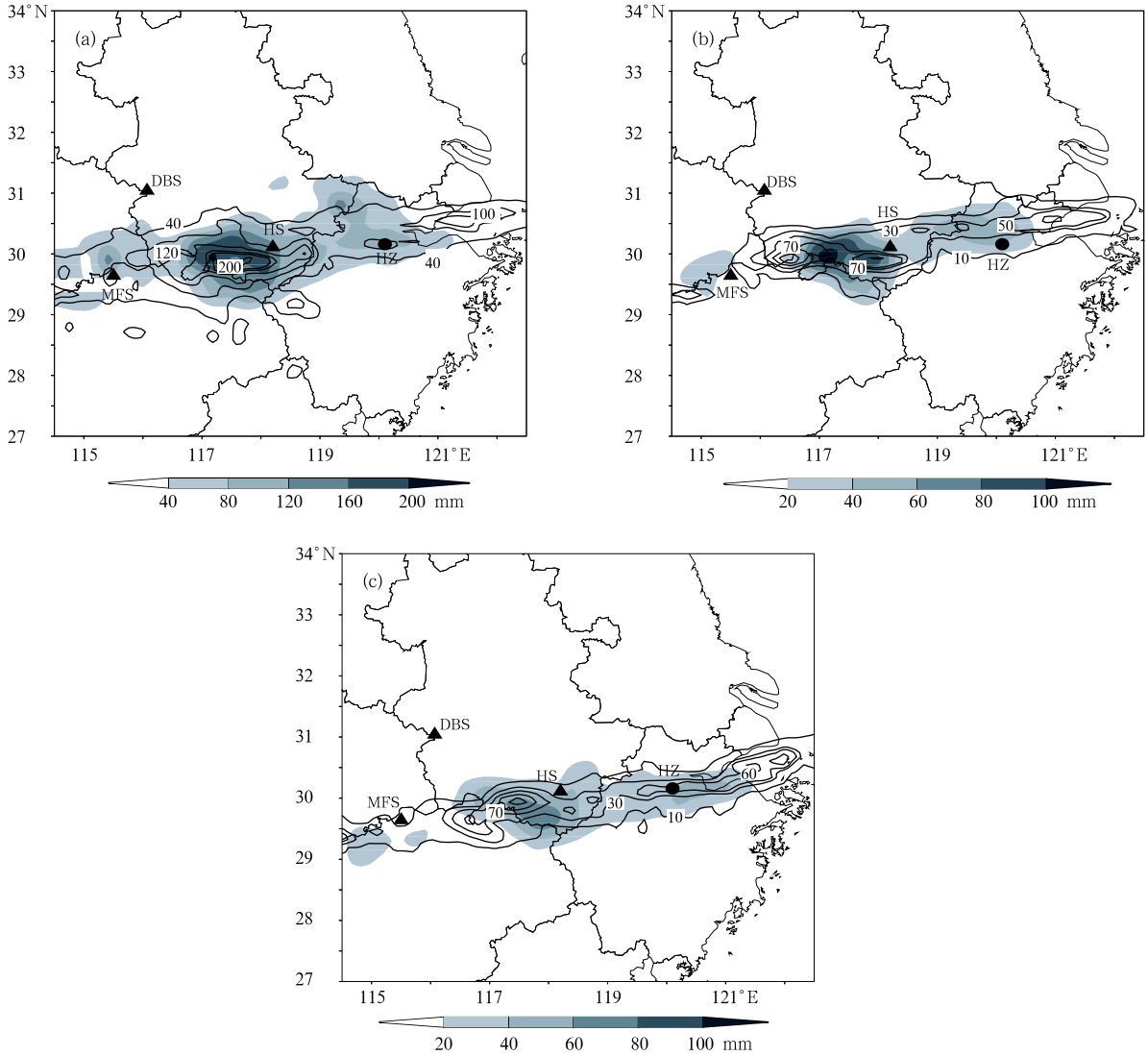

Fig. 6. Observed (shaded) and simulated (contours) accumulative precipitation (a) from 1200 UTC 23 to 1200 UTC 24 July 2009; (b) from 2100 UTC 23 to 0000 UTC 24 July 2009, and (c) from 0000 UTC 24 to 0300 UTC 24 July 2009. HZ represents the city of Hangzhou; DBS, MFS, and HS represent the Dabie, Mufu, and Huang mountains, respectively.

the σ-level ($\sigma = 0.946$) streamline field could be seen at 0200 UTC 24 July (marked "C" in Fig. 8a). The position and horizontal scale of the vortex were found to be close to those in the observed 925-hPa filtered streamline field (Fig. 4a). The observed constant altitude plan position indicator (CAPPI) echo of the Jiujiang Doppler radar at 0100 UTC 24 July 2009 was overlaid in Fig. 8a (shaded). As can be seen, the vortex was accompanied by strong convective activity, with the center of the radar echo band exceeding 50 dBZ. These results suggested that there was an inherent relationship between the PMDV and MCS. They also indicated that there was indeed a PMDV located in the shear line between the center of the observed past hourly accumulative precipitation and the vortex center (Fig. 8b).

The above results illustrate that the simulation generally captured the basic characteristics of the Meiyu frontal rainstorm process and could be used for further analysis.

5.2 Analysis of the PBL streamline field

Analysis of the lower troposphere σ-level fields on 24 July 2009 showed that the vortex was initiated in

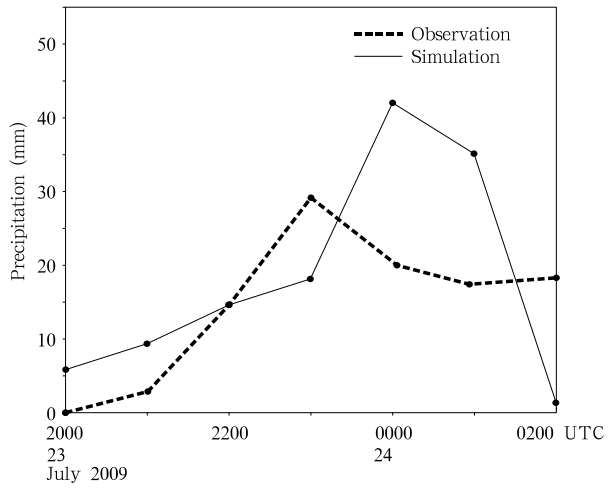

Fig. 7. Observed (dashed) and simulated (solid) past hourly accumulative precipitation (mm) at Dongzhi station.

the PBL and developed upward later. The mesoscale vortex was first clearly observed at the level of $\sigma = 0.946$. A shear line (bold dashed line) was located to the south of Anqing (AQ) and the JHS in the wind field at 2100 UTC 23 July 2009 (Fig. 9a). The south of the shear line was dominated by the meiobar (fine dashed line). Prior to the formation of the PMDV, at 2200 UTC 23 July (Fig. 9b), the region of the meiobar located to the northeast of MFS shrank and became a mesolow when the shear line moved southward. There was a disturbance vortex C_1 located on the southern edge of the mesolow and another disturbance vortex C_2 in the mesolow. We also found that C_2 was close in location to vortex C4 at 2100 UTC 23 July 2009 (Fig. 5d). Meanwhile, an allobaric belt formed to the north of Jinjiang, which was composed of several surface negative allobaric centers (bold solid line) with hourly maximum values of –0.2 hPa. At this time, there was rainfall with hourly accumulative precipitation of about 15 mm in DZ city, as seen from Fig. 7.

With the southward movement of the shear line, the north wind intensified steadily. One hour later (Fig. 9c), the disturbance vortex C_2 kept on strengthening, with the maximum vorticity exceeding 1.2×10^{-3} s^{-1} (shaded), whereas C_1 had already vanished. A new disturbance vortex C_3 with maximum vorticity exceeding 0.8×10^{-3} s^{-1} was generated to the northeast of C_2. A short-term storm also appeared (Fig. 7), with hourly accumulative precipitation of 45 mm (from 2300 UTC 23 to 0000 UTC 24 July 2009) at DZ city, which was in the neighborhood of vortex C_3.

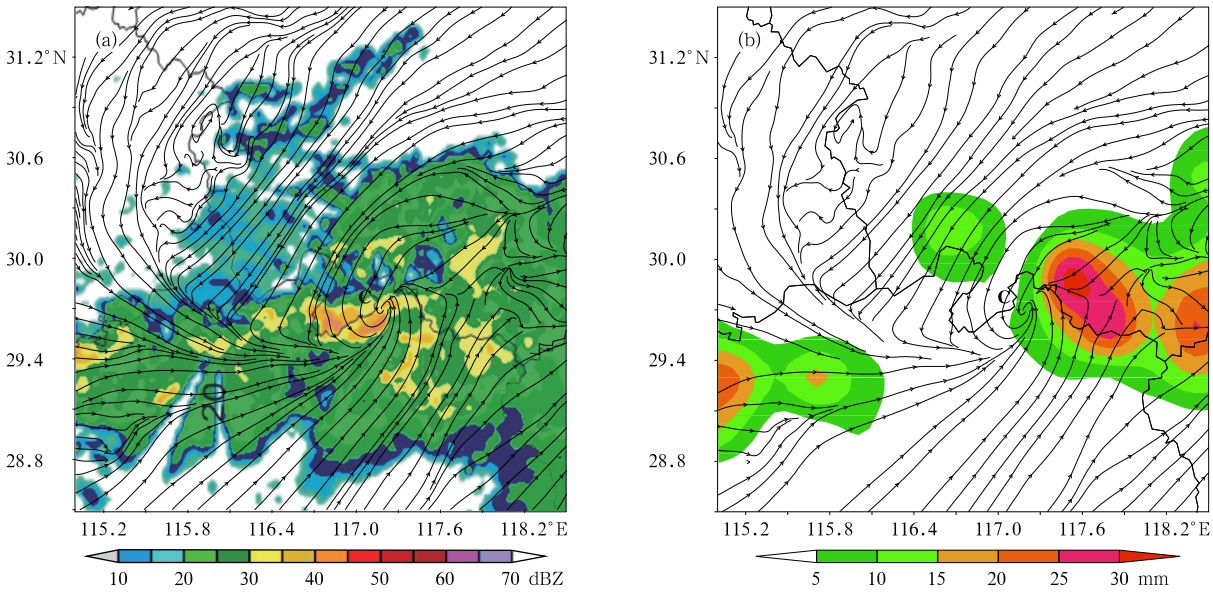

Fig. 8. Simulated streamline fields at $\sigma = 0.946$ at 0200 UTC 24 July 2009 overlaid with (a) the observed CAPPI echo (shaded; dBZ) of the Jiujiang Doppler radar at 0100 UTC 24 July 2009 and (b) the observed past hourly accumulative precipitation (shaded; mm) at 0200 UTC 24 July 2009.

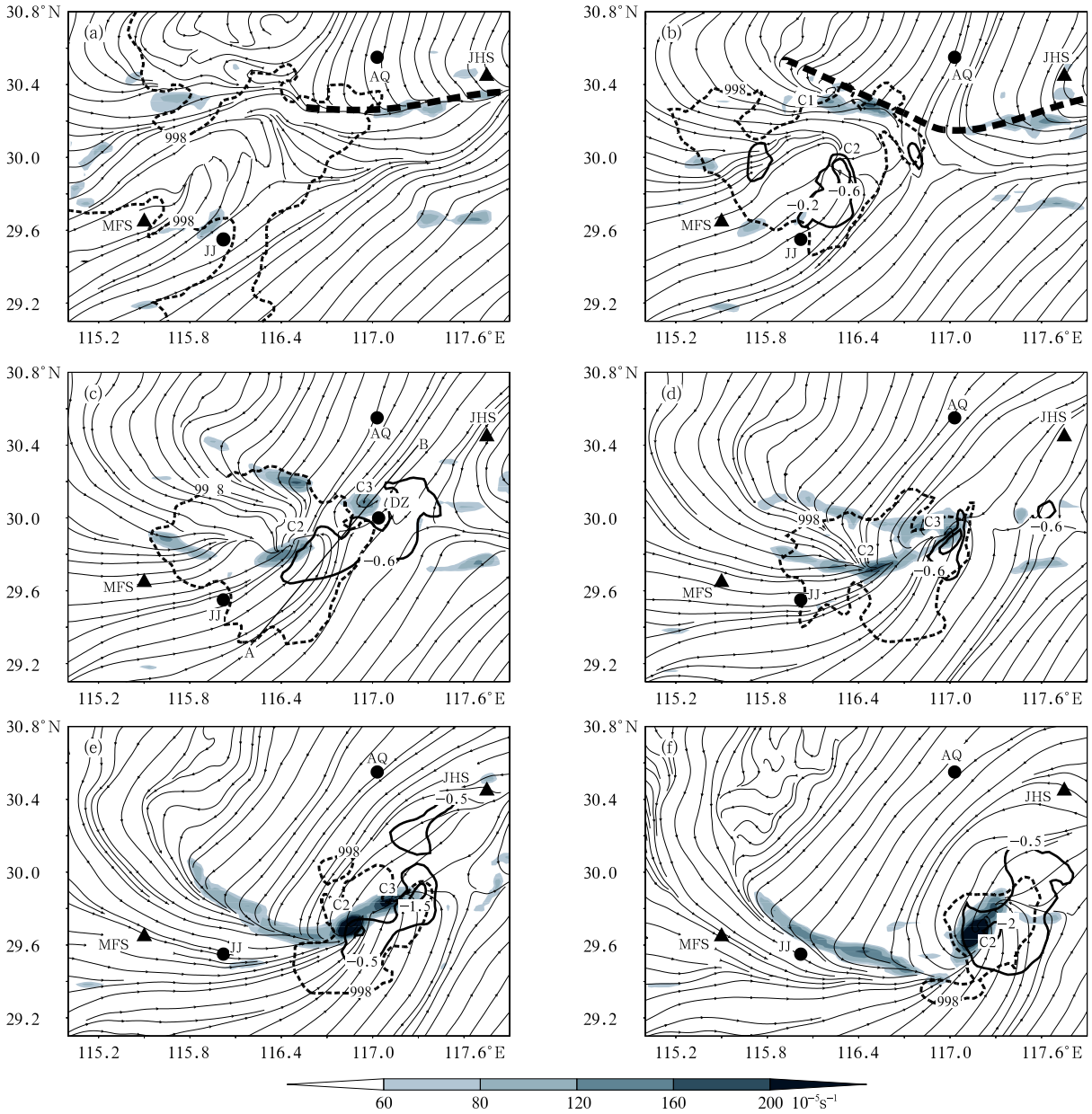

Fig. 9. Simulated streamline fields at $\sigma = 0.946$ at (a) 2100 UTC, (b) 2200 UTC, (c) 2300 UTC 23 July, (d) 0000 UTC, (e) 0100 UTC, and (f) 0200 UTC 24 July 2009. The shading represents vorticity ($\times 10^{-5}$ s^{-1}). The bold solid line indicates the surface allobar during the past one hour (hPa). The fine dashed line indicates the sea level pressure (hPa). The thick dashed line indicates the position of the shear line. JJ, DZ, and AQ indicate the cities of Jiujiang, Dongzhi, and Anqing, respectively. DBS and JHS indicate the Dabie and Jiuhua mountains, respectively.

This suggested that a great increase in precipitation in DZ would have been closely related to vortex C_3. Vortices C_2 and C_3 matched well with the past hourly surface negative allobaric belt. The surface allobar intensified gradually ahead of vortices with a value of –1.2 hPa. The next hourly vorticity centers and vortices occurred over this allobaric belt one hour later (Fig. 9d). At this time, vortex C_2 remained unstable and could not form a closed circulation. Then, vortex C_3 continued to move southward and intensified, with the center value of vorticity reaching 1.2×10^{-3} s^{-1}. There appeared to be a clearly closed center on the streamline field, indicating the formation of the mesoscale vortex C_3.

Later (see in Fig. 9e), vortices C_2 and C_3 continually moved southward, with the hourly surface allobaric belt lying in their front. As the allobaric belt intensified, the vortices gradually enhanced and became attracted to each other. At 0200 UTC 24 July 2009 (Fig. 9f), C_2 merged into C_3 and the surface vortices entered the mature stage. These could all be conducive to the subsequent strong PMDV.

During this process, the development and evolution of the mesoscale vortices were always accompanied by a surface mesolow (fine dashed line in Fig. 9). At the initial stage, the surface mesolow existed before the appearance of the surface vortex, indicating that they were two independent systems. With the development of the vortex, the area of the surface low reduced and the low tended to overlay the surface vortex, which was favorable for the development of low-level divergence and mesoscale convection.

From 0500 to 0800 UTC 24 July 2009, the PMDV continued to move southeastward and began to dissipate (figure omitted). The vortex dominated the area of heavy rain for 10 h from its initiation to its dissipation.

5.3 Analysis of the vertical structure

To investigate the spatial features of the vortex and the influence of the flows at low levels and in the PBL, we analyzed the vertical cross-sections through the center of vortex C_3 (line AB in Fig. 9c).

Figure 10a shows the horizontal wind component parallel to the cross-section (contours) and the divergence (shaded) at 2300 UTC 23 July 2009. There was a strong northeast flow (dashed line) with maximum velocity of 10 m s^{-1} to the right side (north) of the vortex (black triangle) in the PBL. The axis of the flow only reached 950 hPa in height. Meanwhile, the southwest flow (bold solid line) prevailed over the left side (south) of vortex C_3 with the center wind speed of 18 m s^{-1}. The axis of the southwest flow occurred at 850 hPa and was caused by the confluence of the southwest and northeast winds, with a strong convergence center of more than -1.4×10^{-3} s^{-1} in the PBL. Consistent with the convergence, there was a strong "line convection" in the upward area, which could ascend up to the mid troposphere. On the other side of the "line convection", there was a weak downward flow. Convergent and ascending motions occurred on the north side of the vortex in the PBL, but divergent and descending motions occurred on its south side. Hence, there was deep convection and rainfall before vortex C_3 appeared. Figure 10b shows the horizontal wind perpendicular to the cross-section (contours) and the vorticity (shaded) at 2300 UTC 23 July 2009. Southeast wind in the PBL to both sides of the vortex was observed, consistent with the circulation of the vortex at the lower levels. There was a positive vorticity column in the middle of the two southeast flows with a central value of 1.4×10^{-3} s^{-1}. It was located just between the convergence and divergence in the PBL. The surface vortices (C_1, C_2, and C_3) served as a precondition for the subsequent development of the PMDV.

With the enhancement and southward movement of the northeast flow to the north side of the PMDV, the PMDV moved southward accordingly. At 0000 UTC 24 July 2009 when vortex C_3 formed (Fig. 10c), the northeast wind (dashed line) stretched to 600 hPa rapidly with maximum velocity of 10 m s^{-1} in the PBL. This could bring short-term storms and increase the precipitation of the region near the vortex. At the same time, the southeast current (dashed line in Fig. 10d) strengthened gradually. Under the combination of convergence, shear line, and vertical ascending motion, the PMDV intensified to a central value of 2.2×10^{-3} s^{-1} and stretched up to the mid troposphere (shaded in Fig. 10d).

The above analysis demonstrates that there was an intimate relationship between the PMDV and MCS. The meeting of the northern and southwestern flows in the PBL when the mesoscale vortex formed generated a strong mesoscale convergence center in the PBL. Meanwhile, a southwesterly jet located on the top of the PBL to the south side of the vortex reinforced the ascending motion and convergence. Hence, it could be concluded that the PMDV was generated when strong cold air flows north of the shear line encountered the southwestern flow south of the shear line. This was accompanied by an intensive velocity

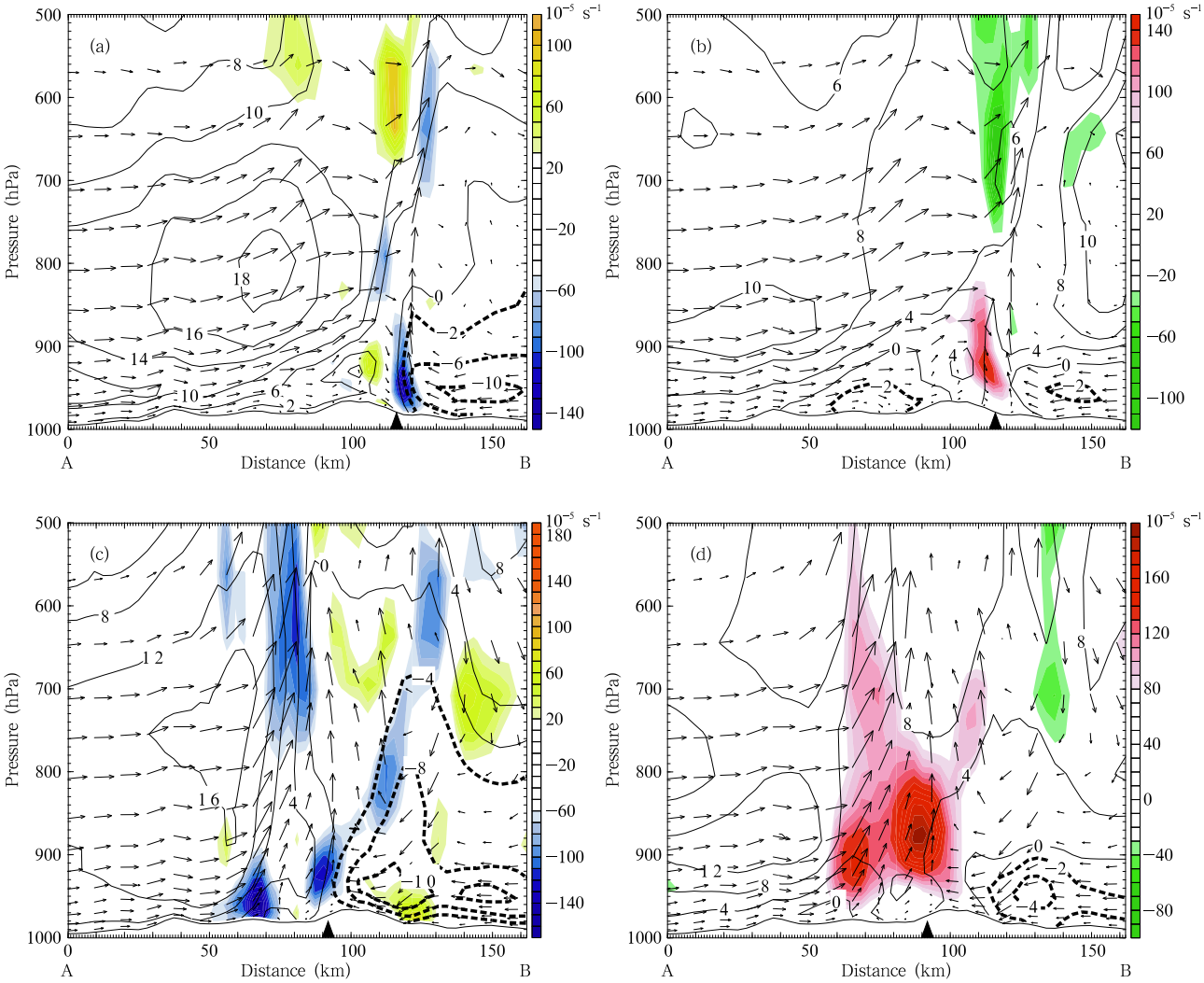

Fig. 10. Vertical cross-sections passing through the vortex C_3 center at (a, b) 2300 UTC 23 July and (c, d) 0000 UTC 24 July 2009. The thick solid and dashed lines in (a, c) indicate the horizontal wind component parallel to the cross-section, while the thick solid and dashed lines in (b, d) indicate the horizontal wind component (m s^{-1}) perpendicular to the cross-section. The colored shading in (a, c) represents the convergence ($\times 10^{-5}$ s^{-1}), while it represents the vorticity ($\times 10^{-5}$ s^{-1}) in (b, d). The black triangle marks the position of vortex C_3. The wind vector indicates the vertical circulation. Line AB can be seen in Fig. 9c.

gradient. This strong convergence could bring a release of instable energy favorable for ascending motion. In return, the PMDV could intensify local convection, bringing about short-term storms over regions near the vortex.

5.4 Thermodynamic factors for the vortex formation

Previous studies have discussed the important role of latent heat in convection (Shi et al., 1996; Zhu et al., 1998; Sun and Zhao, 2002; Sun et al., 2002; Bei et al., 2003). To investigate the influence of latent heat release on the PMDV, we designed a sensitivity experiment in which no latent heat release was allowed (Skamarock et al., 2008). Compared with Fig. 8b, the results show that only large-scale weather systems remained, and the mesoscale convection and vortices disappeared (Fig. 11). The rainfall area extended more widely, but the total rainfall sharply reduced. Obviously, the release of latent heat, which was the crucial

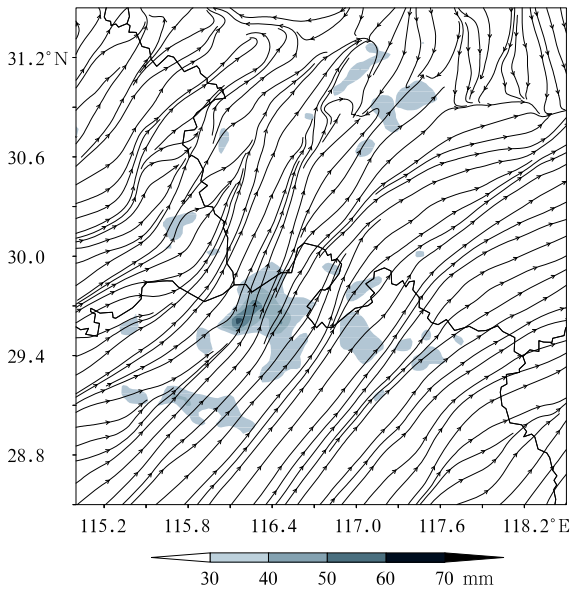

Fig. 11. Simulated streamline fields from the experiment without latent heat at $\sigma = 0.946$ at 0200 UTC 24 July 2009 and 24-h accumulative precipitation (shaded; mm) from 1200 UTC 23 to 1200 UTC 24 July 2009.

thermodynamic factor for the formation of the PMDV, favored the initiation and development of the mesoscale vortex and had a significant impact on the convergence at low levels.

6. Conclusions

The precipitation along Meiyu front is usually unevenly distributed. Sometimes there are one or more disturbance vortices along the shear line. The mesoscale vortices are one of the mesoscale systems that can cause heavy rain. PMDV usually occurs during the development of disturbances. However, these vortices are difficult to be observed as they have small spatial scale, especially at the initial stage.

In order to investigate the detailed characteristics of PMDV, the Shuman-Shapiro smooth filtering method and the ARW model were used to analyze the Meiyu frontal heavy rainfall on 23 July 2009. The model simulation was compared to the automatic weather station data together with Doppler radar data. The results showed that the model could realistically capture the basic characteristics of the mesoscale vortex processes. The main results of this paper are as follows.

(1) Several mesoscale disturbance vortices could be observed in the PBL along the Meiyu front in the lower reaches of the Yangtze River. The vortices in the PBL could be identified clearly in the wind stream field at the initial stage and then they developed upward. One disturbance vortex, with a horizontal scale of about 100 km, was generated in the PBL initially and was responsible for the heavy rainfall over this region. To distinguish it from normal vortices, we called it the PBL mesoscale disturbance vortex (PMDV). By definition, it was different from an MCV, as it was generated in the PBL initially and was accompanied with heavy rainfall.

(2) There were several disturbances along the southern warm section of the Meiyu front. The mesoscale vortices in the PBL interacted with the MCS: the MCS influenced the initiation of vortices; the mesoscale vortices intensified the MCS and the local convective precipitation.

(3) The north and southwest flows in the PBL converged strongly in the PBL at the time of the PMDV formation. Meanwhile, a southwesterly jet on the top of the PBL to the south of the PMDV reinforced the ascending motion and convergence. Hence, it could be concluded that the PMDV was generated when the jet north of the shear line encountered the southwesterly flow south of the shear line. This was accompanied by an intensive velocity gradient. This strong convergence could bring a release of instability energy favorable to ascending motion. The PMDV could intensify local convection by bringing short-term storms over regions near the vortex. Obviously, the convergence line in the PBL, intensification of the southwest wind, and southward aggression of the north wind were important for the development of the PMDV.

(4) The sensitivity experiment that switched off latent heat release manifested that only large-scale weather systems remained, and the mesoscale convection and vortices disappeared. The range of rainfall extended more widely, but the total rainfall sharply reduced. Obviously, the release of latent heat was the crucial thermodynamic factor for the formation of the

PMDV as it had a significant impact on the convergence at low levels.

Acknowledgments. The authors would like to thank Ben and HE Bin for providing the conventional observation data, and the Key Laboratory of Mesoscale Severe Weather (Nanjing University) of Ministry of Education for providing the RSM data. We would also like to thank YIN Jinfang and Professor JIA Xiaojing for improving the manuscript.

REFERENCES

Bartels, D. L., and R. A. Maddox, 1991: Midlevel cyclonic vortices generated by mesoscale convective systems. *Mon. Wea. Rev.*, **119**, 104–118.

Bei Naifang, Zhao Sixiong, and Gao Shouting, 2003: A numerical simulation of sudden heavy rainfall occurred in Wuhan and Huangshi during July 1998. *Chinese J. Atmos. Sci.*, **27**(3), 400–418. (in Chinese)

Brandes, E. A., 1990: Evolution and structure of the 6–7 May 1985 mesoscale convective system and associated vortex. *Mon. Wea. Rev.*, **118**, 109–127.

Cram, T. A., M. T. Montgomery, and R. F. A. Hertenstein, 2002: Early evolution of vertical vorticity in a numerically simulated idealized convective line. *J. Atmos. Sci.*, **59**, 2113–2127.

Davis, C. A., and M. L. Weisman, 1994: Balanced dynamics of mesoscale vortices produced in simulated convective systems. *J. Atmos. Sci.*, **51**, 2005–2030.

Dong Peiming and Zhao Sixiong, 2004: A diagnostic study of mesoscale lows (disturbances) on Meiyu front and associated heavy rainfall. *Chinese J. Atmos. Sci.*, **28**(6), 876–891. (in Chinese)

Dudhia, J., 1989: Numerical study of convection observed during the winter monsoon experiment using a mesoscale two-dimensional model. *J. Atmos. Sci.*, **46**, 3077–3107.

Gao Kun and Xu Yamei, 2001: A simulation study of structure of mesoscale vortices along Meiyu front during 22–30 June 1999. *Chinese J. Atmos. Sci.*, **25**(6), 740–755. (in Chinese)

Grell, G. A., and D. Devenyi, 2002: A generalized approach to parameterizing convection combining ensemble and data assimilation techniques. *Geophys. Res. Lett.*, **29**(14), 1693–1697.

Hong, S. Y., J. Dudhia, and S. H. Chen, 2004: A revised approach to ice microphysical processes for the bulk parameterization of clouds and precipitation. *Mon. Wea. Rev.*, **132**, 103–120.

——, and J. O. J. Lim, 2006: The WRF Single-Moment 6-Class Microphysics Scheme (WSM6). *J. Korean Meteor. Soc.*, **42**, 129–151.

Hu Bowei and Pan Efeng, 1996: Two kinds of cyclonic disturbances and their accompanied heavy rain in the Yangtze River valley during the Meiyu period. *J. Appl. Meteor. Sci.*, **7**(2), 138–144. (in Chinese)

James, E. P., and R. H. Johnson, 2010: Patterns of precipitation and mesolow evolution in midlatitude mesoscale convective vortices. *Mon. Wea. Rev.*, **138**, 909–931.

Janjic, Z. I., 1990: The step-mountain coordinate: Physical package. *Mon. Wea. Rev.*, **118**, 1429–1443.

——, 1996: The surface layer in the NCEP eta model. Eleventh Conference on Numerical Weather Prediction, Norfolk, VA, 19–23 August, Amer. Meteor. Soc., Boston, MA, 354–355.

——, 2002: Nonsingular implementation of the Mellor-Yamada level 2.5 scheme in the NCEP meso model. NCEP Office Note, Report No. 437, 61 pp.

Johnston, E. C., 1981: Mesoscale vorticity centers induced by mesoscale convective complexes. Ninth Conference on Weather Forecasting and Analysis, Seattle, WA, Amer. Meteor. Soc., 196–200.

Knievel, J. C., and R. H. Johnson, 2002: The kinematics of a midlatitude, continental mesoscale convective system and its mesoscale vortex. *Mon. Wea. Rev.*, **130**, 1749–1770.

——, and ——, 2003: A scale-discriminating vorticity budget for a mesoscale vortex in a midlatitude, continental mesoscale convective system. *J. Atmos. Sci.*, **60**, 781–794.

Menard, R. D., and J. M. Fritsch, 1989: A mesoscale convective complex-generated inertially stable warm core vortex. *Mon. Wea. Rev.*, **117**, 1237–1261.

Mlawer, E. J., S. J. Taubman, P. D. Brown, et al., 1997: Radiative transfer for inhomogeneous atmosphere: RRTM, a validated correlated-k model for the longwave. *J. Geophys. Res.*, **102**(D14), 16663–16682.

Olsson, P. Q., and W. R. Cotton, 1997: Balanced and unbalanced circulations in a primitive equation simulation of a midlatitude MCC. Part I: Numerical simulation. *J. Atmos. Sci.*, **54**, 457–478.

Qin Danyu, 2010: A case study of meso-α-scale convective system shape differences using filtering analysis. *Chinese J. Atmos. Sci.*, **34**(1), 154–162. (in Chinese)

Raymond, D. J., and H. Jiang, 1990: A theory for long-lived mesoscale convective systems. *J. Atmos. Sci.*, **47**, 3067–3077.

Schumacher, R. S., and R. H. Johnson, 2008: Mesoscale processes contributing to extreme rainfall in a mid-latitude warm-season flash flood. *Mon. Wea. Rev.*, **136**, 3964–3986.

——, and ——, 2009: Quasi-stationary, extreme-rain-producing convective systems associated with mid-level cyclonic circulations. *Wea. Forecasting*, **24**, 555–574.

Shi Dingpu, Zhu Wenqin, Wang Hongqing, et al., 1996: Cloud top blackbody temperature analysis of infrared satellite image for mesoscale convective system. *J. Appl. Meteor. Sci.*, **54**(5), 600–611. (in Chinese)

Skamarock, W. C., and Coauthors, 2008: A description of the Advanced Research WRF version 3. NCAR Tech. Note, NCAR/TN-475+STR, 125 pp.

Sun Jianhua and Zhao Sixiong, 2002: A study of mesoscale convective systems and its environmental fields during the June 1994 record heavy rainfall in South China. Part II: Effect of physical processes, initial environmental fields and topography on meso-β convective system. *Chinese J. Atmos. Sci.*, **26**(5), 634–646. (in Chinese)

——, Zhang Xiaolin, Qi Linlin, et al., 2002: A study of vortex and its mesoscale convective system during China heavy rainfall experiment and study in 2002. *Chinese J. Atmos. Sci.*, **28**(5), 675–691. (in Chinese)

Sun Suqing and Du Changxuan, 1996: The maintenance of Meiyu front and development associated disturbance. *J. Appl. Meteor. Sci.*, **7**(2), 153–159. (in Chinese)

Tao Zujue, Wang Hongqing, Wang Xu, et al., 1998: A study of meso-α-scale convective systems over China during 1995. *Acta Meteor. Sinica*, **56**(2), 166–177. (in Chinese)

Verlinde, J., and W. R. Cotton, 1990: A mesoscale vortex couplet in the trailing anvil region of a multicellular convective complex. *Mon. Wea. Rev.*, **118**, 993–1010.

Yamada, H., B. Gang, and K. H. Reddy, 2003: Three-dimensional structure of a mesoscale convective system in Baiu-frontal depression generated in the downstream region of the Yangtze River. *J. Meteor. Soc. Japan*, **81**(5), 1243–1271.

Zhai Guoqing, Wang Zhi, and He Bin, 2003: Formation and evolution analysis of the mesoscale vortex group in the middle and lower reaches of the Yangtze River during Meiyu. *Acta Meteor. Sinica*, **61**(6), 661–672. (in Chinese)

——, Zhou Linli, and Wang Zhi, 2007: Analysis of a group of weak small-scale vortices in the planetary boundary layer in the Meiyu front. *Adv. Atmos. Sci.*, **24**(3), 399–408.

Zhang, D. L., 1992: The formation of a cooling-induced mesovortex in the trailing stratiform region of a midlatitude squall line. *Mon. Wea. Rev.*, **120**, 2763–2785.

——, and J. M. Fritsch, 1987: Numerical simulation of the meso-β scale structure and evolution of the 1977 Johnstown flood. Part II: Inertially stable warm-core vortex and the mesoscale convective complex. *J. Atmos. Sci.*, **44**, 2593–2612.

——, and ——, 1988: A numerical investigation of a convectively generated, inertially stable, extratropical warm-core mesovortex over land. Part I: Structure and evolution. *Mon. Wea. Rev.*, **116**, 2660–2687.

Zhang Guocai, Jiao Meiyan, Li Yanxiang, et al., 2007: *Modern Weather Forecasting Technology and Methods.* China Meteorological Press, Beijing, 371 pp. (in Chinese)

Zhang Jin and Tan Zhemin, 2009: A simulation study of the mesoscale convective systems associated with a Meiyu frontal heavy rain event. *Acta Meteor. Sinica*, **23**(4), 438–454.

Zhu Ming, Lu Hancheng, and Yu Zhihao, 1998: Study of positive feedback mechanism for meso-α scale cyclone growing on Meiyu front. *Chinese J. Atmos. Sci.*, **22**(5), 763–770. (in Chinese)

Zhu Qiangen, Lin Jinrong, Shou Shaowen, et al., 2000: *Synoptic Theory and Method.* China Meteorological Press, Beijing, 649 pp. (in Chinese)